Reorientation of the Alkyne Moiety in the Heterometallic Cluster $[FeCo_2(CO)_9(EtC_2Et)]$, induced by Phosphine, Phosphite, or Isonitrile Substitution for CO. Crystal Structure of $[FeCo_2(CO)_8(PPh_3)(EtC_2Et)]$ †

Danilo Boccardo, Mauro Botta, Roberto Gobetto, and Domenico Osella *
Istituto di Chimica Generale ed Inorganica, Università di Torino, Corso Massimo d'Azeglio 48, 10125 Torino, Italy
Antonio Tiripicchio and Marisa Tiripicchio Camellini
Istituto di Chimica Generale ed Inorganica, Università di Parma, Centro di Studio per la Strutturistica Diffrattometrica del C.N.R., Viale delle Scienze, 43100 Parma, Italy

The $[FeCo_2(CO)_9(EtC_2Et)]$ cluster represents the prototype of heterotrimetallic complexes having a *nido*-octahedral structure or in other words a μ_3-(η^2-||) alkyne co-ordination mode. The cluster exhibits a symmetrical (MM||CC) geometry in the solid state; since fluxionality of the alkyne is observed in solution and therefore the rotamers are characterized by subtile energy differences, we have attempted to understand the factors affecting the alkyne orientation over the metallic triangle. The spectroscopic and structural data of the parent cluster have been compared with those of its mono derivatives $[FeCo_2(CO)_8L(EtC_2Et)]$ [L = PEt_3, PPh_3, $P(OMe)_3$, $P(OPh)_3$, or $CNCH_2Ph$]. The structure of $[FeCo_2(CO)_8(PPh_3)(EtC_2Et)]$ has been determined by *X*-ray methods. It crystallizes in the triclinic space group $P\bar{1}$, with $Z = 2$ in a unit cell of dimensions $a = 10.690(4)$, $b = 16.267(8)$, $c = 9.457(5)$ Å, $\alpha = 95.01(3)$, $\beta = 107.55(3)$, and $\gamma = 89.23(2)°$. The structure has been solved from diffractometer data by direct and Fourier methods and refined by full-matrix least squares to $R = 0.0563$ and 4 165 observed reflections. The structure consists of an isosceles triangle of one Fe and two Co atoms. Of the eight carbonyls, seven are terminally bound to the metal atoms [three to Fe, three to the unsubstituted Co(2), one to the Co(1) atom having the phosphine ligand] and one asymmetrically bridges the Fe–Co(1) edge. The EtC_2Et ligand interacts with all three metals, being σ bonded to Fe and Co(2) and π bonded to Co(1) through the triple bond which is disposed nearly parallel to the Fe–Co(2) edge of the cluster. Thus the substitution of a CO for PPh_3 has caused the reorientation of the alkyne moiety in the ground state. Finally, dimers of formula $[\{FeCo_2(CO)_8(EtC_2Et)\}_2\{Ph_2P(CH_2)_nPPh_2\}]$ ($n = 2$—4) have been characterized by means of multinuclear n.m.r. spectroscopy.

The rich chemistry of alkyne transition-metal clusters offers a wide range of co-ordination modes, which serve as good models for chemisorbed hydrocarbons on metallic surfaces.[1] As far as alkyne–trimetallic compounds are concerned, two different bonding modes have been found. In the unsaturated (46-electron) $[Fe_3(CO)_9(RC_2R)]$ (R = alkyl) series[2] the alkyne is observed to be orthogonal to an iron–iron edge, namely μ_3-(η^2-⊥); on the other hand in the saturated (48-electron) $[M_3H_2(CO)_9(RC_2R)]$ (M = Ru or Os) clusters[3] the triple bond is parallel to a metal–metal edge, namely μ_3-(η^2-||) according to the notation of Muetterties and co-workers.[4]

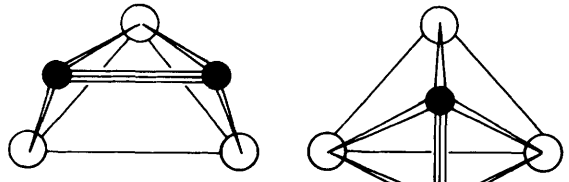

μ_3-(η^2-||) μ_3-(η^2-⊥)

† 2,3-μ-Carbonyl-1,1,1,2,3,3,3-heptacarbonyl-μ_3-[hex-3-yne-C^3(Co^2Fe^3)C^4($Co^{1,2}$)]-2-triphenylphosphine-*triangulo*-dicobaltiron.

Supplementary data available: see Instructions for Authors, *J. Chem. Soc., Dalton Trans.*, 1988, Issue 1, pp. xvii—xx.

In detailed extended-Hückel molecular orbital (EHMO) studies Schilling and Hoffmann[5] and subsequently Jaouen and co-workers[6] rationalized the preference for the perpendicular and parallel orientation in the model complexes $[Fe_3(CO)_9(HC_2H)]$ and $[Fe_3(CO)_9(HC_2H)]^{2-}$ respectively as a consequence of the different energies of the frontier orbitals. In a recent study of the electrochemical behaviour of the $[Fe_3(CO)_9(RC_2R)]$ series, we have shown the occurrence of a fully reversible $\perp \rightleftharpoons \parallel$ interconversion *via* a two-electron redox process.[7] The molecular orbital energy level sequence and symmetry have been confirmed, with minor differences, by two CNDO calculations and furthermore the tendency of tri-iron clusters to afford 46-electron systems and triruthenium and triosmium clusters to give 48-electron complexes when reacted with alkynes has been rationalized on the basis of the different electronegativities of the metals.[8] In terms of the polyhedral skeletal electron pair approach,[9] the two acetylene orientations can be explained as the result of two different polyhedral shapes: the six-electron pair *closo* trigonal bipyramid (⊥) and the seven-electron pair *nido* octahedron (||).

Within the μ_3-(η^2-||) co-ordination mode, different structures can occur when the symmetry of the triangle is lowered by the use of different metals. Indeed the solid-state structure determinations of several *nido* M_2M'–alkyne clusters have shown that both symmetrical (MM||CC) and asymmetrical (MM'||CC) geometries can be found.[6] The difference in energy of the possible isomers has been evaluated to be very small and in the case of $[W_2Os(CO)_7(\eta\text{-}C_5H_5)(RC_2R)]$ (R = C_6H_4Me-4) both possible rotamers are present in the crystal.[10] Actually,

fluxionality of the alkyne is expected in solution, so that several isomers may co-exist in equilibrium and subtile energy differences may favour one of them when crystallization is occurring. Jaouen and co-workers[6] have carried out an exhaustive EHMO study and indicated that the thermodynamically preferred rotamer should have the more electronegative metal fragments located in the 'basal or parallel' edge rather than in the apical vertex of the *nido* polyhedron. This explains the different structures adopted by $[FeCo_2(CO)_9(EtC_2Et)]$[11] and $[RuCo_2(CO)_9(PhC_2Ph)]$:[12] the former complex has a symmetrical (CoCo‖CC) geometry and the latter an asymmetrical (CoRu‖CC) one as expected on the basis of Pauling's electronegativity values (Fe ≤ Co < Ru).

It is noteworthy that the asymmetrical structure shows a semibridging CO group, which plays an important role in the synergic mechanism of charge redistribution from the electron rich Co (19-electron) to the electron poor Ru (17-electron) atom, according to Cotton's proposal.[13]

A similar trend has been found by Sutton and co-workers[14] in the heterotrimetallic $[NiCoM(CO)_6(\eta\text{-}C_5H_5)(RC_2R)]$ (M = Fe, Ru, or Os) series. It has been suggested that the substitution of a carbonyl group by a phosphine should vary the electron density at the metal and hence stabilize a different isomer.[6] Indeed in $[NiCoFe(CO)_6(\eta\text{-}C_5H_5)(RC_2R)]$ clusters a change in the orientation of the alkyne from a position parallel to the Ni–Co vector (R = Et) to a position parallel to the Ni–Fe edge (R = Ph) has been found as a consequence of the *formal* substitution of PPh_3 for CO on the $Co(CO)_3$ moiety.[14] Unfortunately in this example, the reported clusters possess different substituted alkynes and this may alter the ground-state energies. An example of the effect of the alkyne substituents

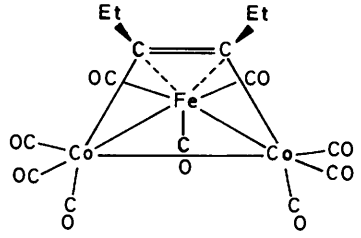

$[FeCo_2(CO)_9(EtC_2Et)]$

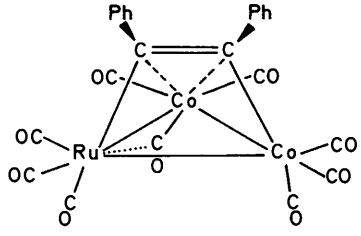

$[RuCo_2(CO)_9(PhC_2Ph)]$

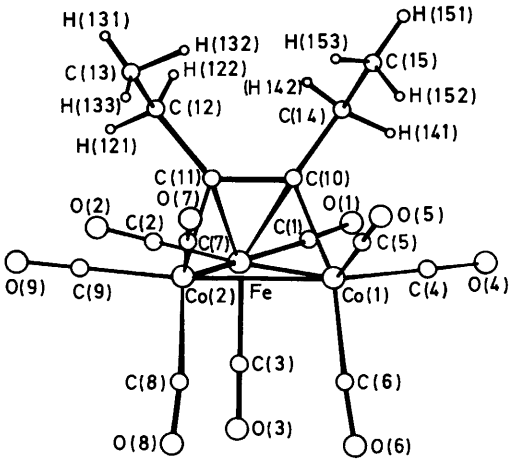

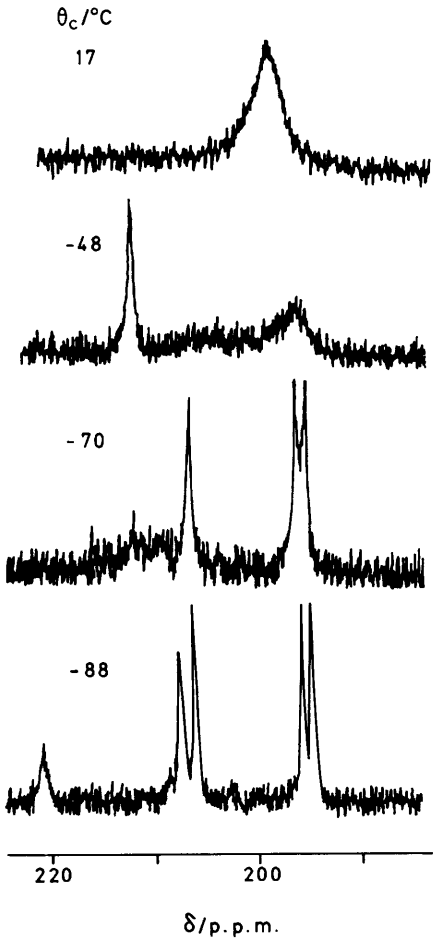

Figure 1. Variable-temperature ^{13}C n.m.r. spectra of a ^{13}CO-enriched sample of $[FeCo_2(CO)_9(EtC_2Et)]$ (**1**) recorded at 67.9 MHz in $CDCl_3$, together with the view of its solid-state structure (ref. 11)

can be found when the different solid-state structures of $[Os_3(CO)_{10}(PhC_2Ph)]$ and $[Os_3(CO)_{10}(EtC_2Et)]$ are considered.[15]

In an attempt to evaluate the electronic and steric influence of external ligands on the alkyne orientation, we have brought about the substitution of one CO group in $[FeCo_2(CO)_9(EtC_2Et)]$ (**1**) by different, σ-donor/π-acceptor ligands, namely PEt_3, PPh_3, $P(OMe)_3$, $P(OPh)_3$, CN, $CNCH_2Ph$, 1,2-bis(diphenylphosphino)ethane (dppe), 1,3-bis(diphenylphosphino)propane (dppp), and 1,4-bis(diphenylphosphino)butane (dppb).

Results and Discussion

Syntheses.—The overall structure of $[FeCo_2(CO)_9(EtC_2Et)]$ (**1**) was determined by *X*-ray analysis[11] although the position of the metal atoms in the cluster could not be ascertained unambiguously because of the small difference in the scattering power of Fe and Co atoms. The variable-temperature ^{13}C n.m.r. spectra (at 2.3 T) supported the symmetrical (CoCo‖CC) geometry, although the low-temperature limiting spectrum was of poor quality because of the low solubility of the sample.[11]

We have repeated the variable-temperature ^{13}C n.m.r. study at higher field (6.4 T) as shown in Figure 1. At −88 °C the observed resonances are fully consistent with the suggested structure: the low-field resonances at 220.8 and 207.4 p.p.m. of integrated intensity ratio 1:2 are assigned to the axially and equatorially iron-bound carbonyls respectively, the other resonances of intensity ratio 2:2:2 to the three sets of carbonyls on the cobalt atoms. As previously proposed, three exchange processes take place: (*i*) localized scrambling at the $Fe(CO)_3$ moiety, (*ii*) localized scambling at the $Co(CO)_3$ units, and (*iii*) total CO exchange over the metallic triangle through a 'merry-go-round' process which is probably coupled with the alkyne rotation.

The variable-temperature ^1H n.m.r. spectra indicate that the rotation of the alkyne ligand over the metallic plane is occurring in the temperature range +25 to −50 °C since the quartet at 2.57 p.p.m. (two equivalent methylene groups) remains unchanged. If the alkyne were static, two different AB patterns should be observed for the $-CH_2$ groups, since they are diastereotopic as a consequence of their proximity to the chiral acetylene carbons.[16]

Having a firm knowledge of the ground-state structure and dynamic behaviour of the parent compound (**1**), we proceeded to synthesize the monosubstituted derivatives $[FeCo_2(CO)_8L(EtC_2Et)]$ (**2**) [L = PEt_3, PPh_3, $P(OMe)_3$, $P(OPh)_3$, or $CNCH_2Ph$]. Since (**1**) is only moderately stable, the thermal activation resulted in extensive cluster fragmentation and consequently low yields of the desired products. To circumvent this problem, the dimer $[\{Fe(CO)_2(PPh_3)(SMe)\}_2]$ was employed as a catalyst. This complex has been proved to be a very versatile catalyst for carbonyl substitution in transition-metal clusters *via* the generation of active radical species in solution[17] (Figure 2). By using $[\{Fe(CO)_2(PPh_3)(SMe)\}_2]$ in a 1:10:10 mol ratio with respect to cluster (**1**) and a suitable ligand (L) the substitution reactions occur quickly at room temperature giving rise to high yields (70—90%) of monosubstituted derivatives according to equation (1).

$$[FeCo_2(CO)_9(EtC_2Et)] + L \xrightarrow{\text{catalyst}} [FeCo_2(CO)_8L(EtC_2Et)] + CO \quad (1)$$

(**1**)

L

(**2a**) PEt_3
(**2b**) PPh_3
(**2c**) $P(OMe)_3$
(**2d**) $P(OPh)_3$
(**2e**) $CNCH_2Ph$

The compounds gave acceptable elemental analyses (Table 1); only in the cases of $[FeCo_2(CO)_8\{P(OMe)_3\}(EtC_2Et)]$ (**2c**) and $[FeCo_2(CO)_8(CNCH_2Ph)(EtC_2Et)]$ (**2e**) were the samples volatile enough to obtain mass spectra in the available electron-impact mode. As in the parent compound (**1**),[11] the molecular ion peaks for both complexes are extremely low in intensity; for (**2c**) the highest peak corresponds to $[FeCo_2(CO)_7\{P(OMe)_3\}(EtC_2Et)]^+$, while for (**2e**) to $[FeCo_2(CO)_8(EtC_2Et)]^+$. An *X*-ray analysis of (**2b**), which gave the best shaped crystals, was undertaken to assess the molecular structure of these compounds.

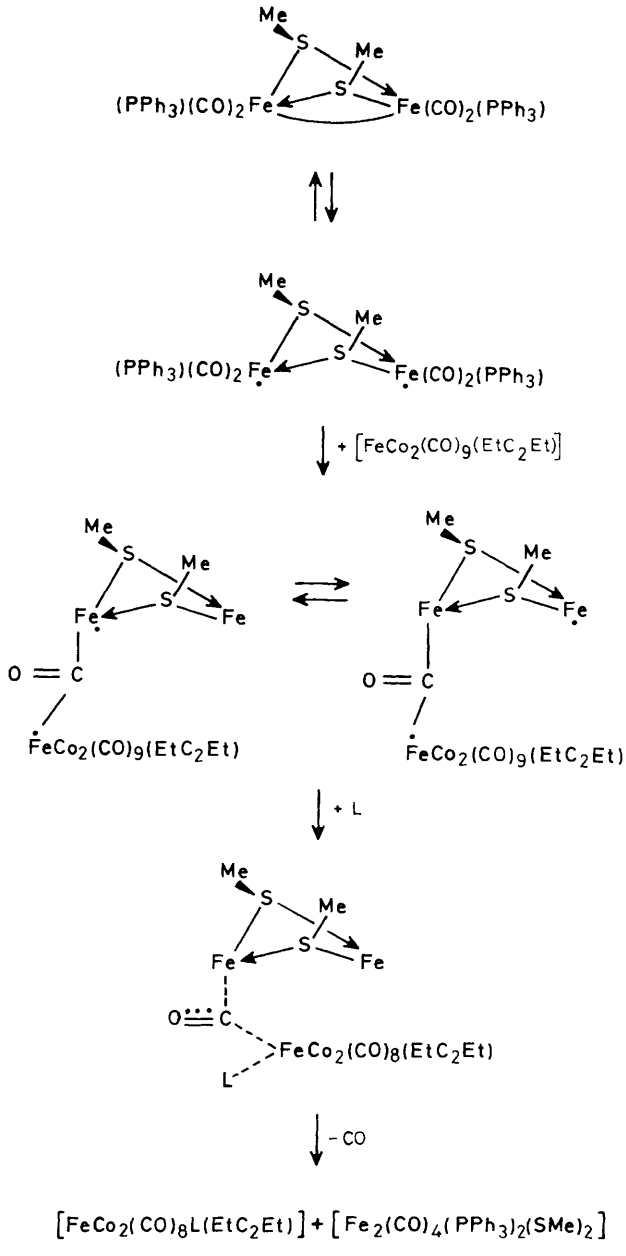

Figure 2. Proposed mechanism of CO substitution in $[FeCo_2(CO)_9(EtC_2Et)]$ (**1**) catalyzed by $[\{Fe(CO)_2(PPh_3)(SMe)\}_2]$. For further details see ref. 17

Crystal Structure of $[FeCo_2(CO)_8(PPh_3)(EtC_2Et)]$ (**2b**).—The structure of (**2b**) is represented in Figure 3 together with the atomic labelling system. Selected bond distances and angles are given in Table 2. The complex consists of an isosceles triangle of two Co and one Fe atoms. (See Experimental section for

Table 1. Chemical analyses and i.r. data of the synthesized compounds

Complex	Physical state	Found (calc.) (%) Fe	Co	C	H	ν(CO)[a]/cm^{-1}
(**2a**)	Green solid	9.4 (9.35)	19.5 (19.70)	39.7 (40.15)	4.3 (4.20)	2 072s, 2 028vs, 2 016s, 2 006s, 1 980w, 1 962m, 1 877w br
(**2b**)	Green solid	7.7 (7.50)	15.6 (15.90)	51.3 (51.80)	3.5 (3.40)	2 072s, 2 030vs, 2 018s, 2 007m, 1 990w br, 1 981m br, 1 876 br w
(**2c**)	Brown oil	9.4 (9.25)	19.7 (19.50)	39.4 (33.80)	3.2 (3.20)	2 075s, 2 032vs, 2 018s, 2 010s, 1 986w, 1 977m br, 1 878 br w
(**2d**)	Brown oil	7.5 (7.05)	14.4 (14.90)	48.2 (48.65)	3.3 (3.20)	2 077s, 2 034vs, 2 021s, 2 012s, 1 984m, 1 974w, 1 867 br w
(**2e**)	Brown solid	9.5 (9.35)	20.1 (19.75)	44.7 (44.25)	3.0 (2.90)	2 169s,[b] 2 075s, 2 033vs, 2 030vs, 2 024vs, 2 011m, 2 007w, 1 999m, 1 964m, 1 957w, 1 876vw
(**3a**)	Green solid	6.2 (6.35)	13.1 (13.40)	54.5 (54.70)	4.1 (3.90)	2 071s, 2 030vs, 2 016s, 2 006m, 1 980m, 1 962m, 1 870 br w
(**3b**)	Green solid	6.1 (6.25)	13.4 (13.20)	54.9 (55.20)	4.2 (4.05)	2 072s, 2 029vs, 2 016s, 2 007s, 1 979m, 1 970m, 1 868br w
(**3c**)	Green solid	6.2 (6.15)	13.1 (13.00)	54.1 (55.65)	4.4 (4.25)	2 072s, 2 029vs, 2 017s, 2 007s, 1 978m, 1 971w, 1 866w

[a] In n-hexane. [b] ν(C≡N).

Table 2. Selected bond distances (Å) and angles (°)

(*a*) Metal co-ordination spheres

Co(1)–Co(2)	2.448(2)	Fe–C(3)	1.778(7)
Co(1)–Fe	2.476(2)	Fe–C(4)	1.805(9)
Co(2)–Fe	2.623(2)	Fe–C(5)	1.744(8)
Co(1)–P	2.210(2)	Fe–C(9)	2.019(8)
Co(1)–C(1)	1.738(6)	Co(2)–C(6)	1.805(10)
Co(1)–C(2)	1.797(7)	Co(2)–C(7)	1.773(8)
Co(1)–C(9)	2.038(7)	Co(2)–C(8)	1.836(9)
Co(1)–C(10)	2.078(6)	Co(2)–C(10)	1.981(7)
Fe–C(2)	2.233(7)		
Fe–Co(1)–Co(2)	64.4(1)	C(1)–Co(1)–C(2)	104.9(3)
Fe–Co(2)–Co(1)	58.3(1)	C(3)–Fe–C(4)	96.0(4)
Co(1)–Fe–Co(2)	57.3(1)	C(3)–Fe–C(5)	94.4(4)
Fe–Co(1)–P	127.7(1)	C(4)–Fe–C(5)	96.7(4)
Co(2)–Co(1)–P	165.4(1)	C(6)–Co(2)–C(7)	104.3(4)
P–Co(1)–C(1)	91.0(3)	C(6)–Co(2)–C(8)	96.3(4)
P–Co(1)–C(2)	96.3(2)	C(7)–Co(2)–C(8)	97.4(4)

(*b*) Carbonyl groups

C(1)–O(1)	1.140(9)	C(5)–O(5)	1.149(10)
C(2)–O(2)	1.138(10)	C(6)–O(6)	1.132(13)
C(3)–O(3)	1.138(9)	C(7)–O(7)	1.127(10)
C(4)–O(4)	1.129(13)	C(8)–O(8)	1.105(11)
Co(1)–C(1)–O(1)	176.2(8)	Fe–C(4)–O(4)	178.1(7)
Co(1)–C(2)–O(2)	156.8(7)	Fe–C(5)–O(5)	178.7(8)
Fe–C(2)–O(2)	128.2(6)	Co(2)–C(6)–O(6)	178.0(9)
Co(1)–C(2)–Fe	74.9(2)	Co(2)–C(7)–O(7)	176.8(8)
Fe–C(3)–O(3)	176.1(8)	Co(2)–C(8)–O(8)	176.2(9)

(*c*) Other ligands

P–C(15)	1.809(6)	C(9)–C(11)	1.519(9)
P–C(21)	1.822(8)	C(11)–C(12)	1.516(10)
P–C(27)	1.827(7)	C(10)–C(13)	1.510(11)
C(9)–C(10)	1.367(8)	C(13)–C(14)	1.560(12)
Co(1)–P–C(15)	116.8(2)	C(15)–P–C(27)	100.9(3)
Co(1)–P–C(21)	112.1(2)	C(21)–P–C(27)	103.7(3)
Co(1)–P–C(27)	116.6(2)	C(11)–C(9)–C(10)	127.7(6)
C(15)–P–C(21)	105.2(3)	C(9)–C(10)–C(13)	126.5(6)

attempts to discriminate between Fe and Co atoms.) Seven carbonyl groups [three on Co(2) and Fe, one on Co(1)] are terminally bound to the metals, whilst one semibridges Co(1) and Fe [Co(1)–C(2) 1.797(7), Fe–C(2) 2.233(7) Å,

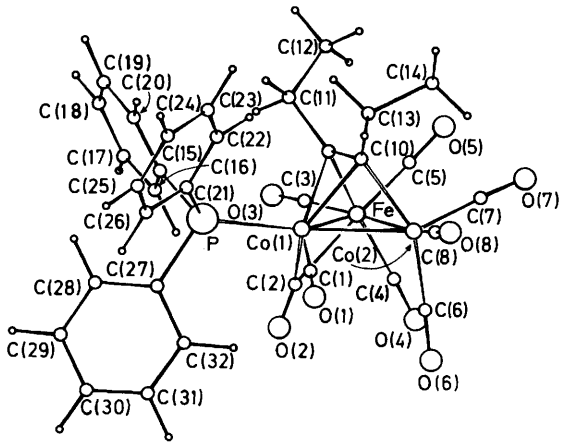

Figure 3. View of the molecular structure of $[FeCo_2(CO)_8(PPh_3)(EtC_2Et)]$ (**2b**) with the atomic numbering scheme

Co(1)–C(2)–O(2), 156.8(7)°]. The PPh_3 ligand is bound to Co(1) and occupies an equatorial position. The hex-3-yne ligand interacts with all three metals, being bonded to Co(2) and Fe *via* σ interactions [Co(2)–C(10) 1.981(7) and Fe–C(9) 2.019(8) Å] and to Co(1) in a π fashion [Co(1)–C(9) 2.038(7) and Co(1)–C(10) 2.078(6) Å]. The alkyne–metal bonding is thus of the μ_3-(η^2-‖) type with the acetylenic C–C bond [C(9)–C(10) 1.367(8) Å] parallel to the Co(2)–Fe edge, the longest of the cluster [Co(2)–Fe 2.623(2), Co(1)–Co(2) 2.448(2), and Co(1)–Fe 2.476(2) Å]. This situation has been found previously in $[RuCo_2(CO)_9(PhC_2Ph)]$ [12] in which the acetylenic C–C bond, of length 1.370(3) Å, is nearly parallel to one Ru–Co edge of the cluster, the longest [2.6875(5) *versus* 2.5865(5) (Ru–Co) and 2.4535(5) Å (Co–Co)], and with a semibridging carbonyl between the Ru–Co edge not parallel to the C–C bond.

The structure of (**2b**) can also be compared with that of (**1**) from which one carbonyl has been substituted by one PPh_3 ligand. This substitution determines a change in the orientation of the triple C–C bond, which in (**1**) is parallel to the Co–Co edge [always the longest, 2.576(1) *versus* 2.479(1) and 2.489(1) Å of the Fe–Co edges], and the transformation of a terminal carbonyl into a semibridging carbonyl.

Furthermore the entry of the bulky PPh_3 ligand causes some

Table 3. N.m.r. data of the synthesized compounds

Complex	^{31}P-{^1H}[a]/p.p.m.	^1H[b]/p.p.m.	^{13}C-{^1H}[c]/p.p.m.
(**2a**)	38.8	C_2H_5P: 1.43 (m, 6), 1.07 (m, 9) $C_2H_5C_2$: 3.02—1.80 (m br, 4), 1.68 (m, 6)	CO: 210.4;[d] C_2: 173.3, 164.0; $C_2H_5C_2$: 39.5, 38.2, 18.5, 17.9; C_2H_5P: 18.6 (d) (J_{CP} 24 Hz), 7.3 (d) (J_{CP} 2 Hz)
(**2b**)	30.0	Ph: 7.25 (m, 15) CH_2: 2.20—1.25 (m br, 4) CH_3: 1.14 (m, 6)	CO: 208.8;[d] C_2: 173.2, 165.4; Ph: 133.3—128.4; CH_2: 39.4, 37.9; CH_3: 18.6, 17.5
(**2c**)	153.9	CH_3OP: 3.64 (d, 9) (J_{HP} 11.7 Hz) CH_2: 3.09—1.97 (m, 4) CH_3: 1.43 (m, 6)	CO: 207.5;[d] 176.1, 165.3; CH_3PO: 52.3; CH_2: 39.7, 38.0; CH_3: 18.3, 17.7
(**2d**)	140.8	Ph: 7.27 (m, 15) CH_2: 3.05—1.07 (m br, 4) CH_3: 1.09 (m, 6)	CO: 208.5;[d] C_2: 176.2, 164.4; Ph: 151.3—121.2; CH_2: 39.2, 38.5; CH_3: 18.2, 17.9
(**2e**)		Ph: 7.38 (m, 5) CH_2Ph: 4.87 (s, 2) CH_2: 3.10—2.31 (m br, 4) CH_3: 1.39 (m, 6)	CO: 207.1;[d] C_2: 170.2, 168.3; Ph: 131.7—128.9; CH_2: 48.6; C_2H_5: 39.3, 38.3, 18.0, 17.7
(**3a**)	42.9	Ph: 7.40 (m, 20) CH_2: 2.50—1.22 (m br, 8) CH_3: 1.14 (m, 6)	CO: 208.6;[d] C_2: 173.4, 164.1; Ph, 132.5—128.3; C_2H_5: 39.2, 37.7, 18.4, 17.8; $(CH_2)_2$: 30.0—22.3
(**3b**)	38.6	Ph: 7.40 (m, 20) CH_2: 2.48—1.20 (m, 10) CH_3: 1.14 (m, 6)	CO: 208.8;[d] C_2: 173.3, 164.2; Ph: 132.6—128.4; C_2H_5: 39.1, 37.7, 18.3, 17.8; $(CH_2)_3$: 30.1—22.0
(**3c**)	39.5	Ph: 7.40 (m, 20) CH_2: 2.60—1.21 (m br, 12) CH_3: 1.15 (m, 6)	CO: 208.9;[d] C_2: 173.8, 164.2; Ph: 132.7—128.5; C_2H_5: 39.2, 37.6, 18.3, 17.7; $(CH_2)_4$: 30.2—22.1

[a] $CDCl_3$, chemical shifts relative to 85% H_3PO_4. [b] $CDCl_3$, chemical shifts relative to $SiMe_4$. [c] CD_2Cl_2, chemical shifts relative to $SiMe_4$. [d] Coalescence obtained at the following temperatures: (**2a**) +38 °C; (**2b**) +50 °C; (**2c**) +30 °C; (**2d**) +34 °C; (**2e**) +27 °C; (**3a**), (**3b**), and (**3c**) *ca.* 45 °C.

deviations in the carbonyls. Obviously the most significant differences concern the carbonyls at Co(1) as indicated by the corresponding angles [the two values refer to the complexes (**1**) and (**2b**) respectively]: Fe–Co(1)–C(2), 91.0(2) *vs.* 60.6(2), Co(2)–Co(1)–C(2), 91.7(3) *vs.* 97.4(3), C(1)–Co(1)–C(2), 96.0(4) *vs.* 104.9(3), C(1)–Co(1)–Fe, 162.3(3) *vs.* 138.0(3), and C(1)–Co(1)–C(2) 100.9(3) *vs.* 80.5(3) Å.

As in (**1**) the C(9)C(10)FeCo(2) group is planar and C(11) and C(13) are displaced from this plane by 0.157(7) and 0.404(8) Å respectively; the C(9)C(10)C(11)C(13) moiety is also planar, with the plane passing through them inclined by 72° to the cluster triangle.

Solution Structure and Dynamics.—Regiospecific substitution of a carbonyl by a Group 5 ligand on a $Co(CO)_3$ moiety has been found in other iron–cobalt compounds, such as $[FeCo_2(CO)_9(S)]$,[18] $[FeCo_3H(CO)_{12}]$,[19] and $[FeCo(CO)_6(R_2CC{\equiv}CR')]$ (R,R′ = alkyl).[20]

The ligand substitution on a $Co(CO)_3$ unit is further corroborated by the large ^{31}P linewidth at half height in (**2b**) ($\nu_{\frac{1}{2}}$ *ca.* 55 Hz at 22 °C), broadening being due to the quadrupole effect of the neighbouring Co atom; the resonance for the same PPh_3 ligand bonded to an iron centre should be narrower, *i.e.* $\nu_{\frac{1}{2}}$ *ca.* 15 Hz at 22 °C for $[Fe_3(CO)_{11}(PPh_3)]$.[21]

The i.r. spectra of all the monosubstituted derivatives exhibit a very similar pattern in hexane solution suggesting the presence of a single rotamer. The occurrence of a semibridging CO group is confirmed by the weak absorptions in the expected range of 1 880—1 860 cm^{-1} (Table 1). The small differences in wavelengths can be easily related to the different σ-donor/π-acceptor properties of the corresponding ligands.[22]

As a consequence of the replacement of CO on $Co(CO)_3$ by L, the organometallic clusters possess an inherent chirality due to the three different metallic centres. This causes the occurrence of four magnetically non-equivalent protons for the two diastereotopic methylene groups whether the alkyne rotation over the metallic triangle takes place or not. Thus four signals can be expected and are experimentally found in the CH_2 region of the ^1H n.m.r. spectra of all the mono derivatives, along with two methyl triplets. The methylene signals appear as very complex multiplets because of coupling to the adjacent CH_3 group, the geminal proton, and the phosphorus atom of the ligand [(**2a**)—(**2d**) only].

Unfortunately the CH_2 multiplets and the CH_3 triplets are partially superimposed (at least at 6.4 T) so that the assignment of the proton resonance within each ethyl group was impossible by selective decoupling.[14]

The ^{13}C-{^1H}-n.m.r. spectra in the organic region further corroborated the FeCo‖CC asymmetric structure: for all the mono derivatives two acetylene, two methylene, and two methyl resonances are observed at room temperature (Table 3).

The low-temperature limiting ^{13}C n.m.r. spectra in the carbonyl region of ^{13}CO-enriched samples of (**2a**)—(**2c**) are very similar and fully consistent with the solid-state structure found for (**2b**). For example, for (**2b**) seven resonances are found at −75 °C at 232.1 (s), 212.3 (s), 210.6 (s), 209.4 (d, J_{CP} 22.3 Hz), 206.2 (s), 203.0 (s), and 198.8 (s) p.p.m. in an integrated intensity ratio of 1:1:1:1:1:1:2. The low-field peak is straightforwardly assigned to the semibridging CO group and the doublet to the unique carbonyl bound to the substituted cobalt centre (Figure 4). The remaining resonances are attributed to the Fe- (212.3 and 210.6 p.p.m.) or Co-bound carbonyls on the basis of their chemical shift values (generally higher for Fe–CO than for Co–CO);[23] moreover as the temperature is raised the resonances of the Co–CO groups become broader, as the thermal decoupling is less effective.[24]

At 0 °C the two upfield peaks coalesce and merge to a single resonance at *ca.* 201 p.p.m., indicating a localized scrambling within the $Co(1)(CO)_3$ moiety. At this temperature all the other resonances except that at 210.6 p.p.m. start to broaden. While it is difficult to differentiate between quadrupolar broadening and exchange broadening for the semibridging and terminal cobalt

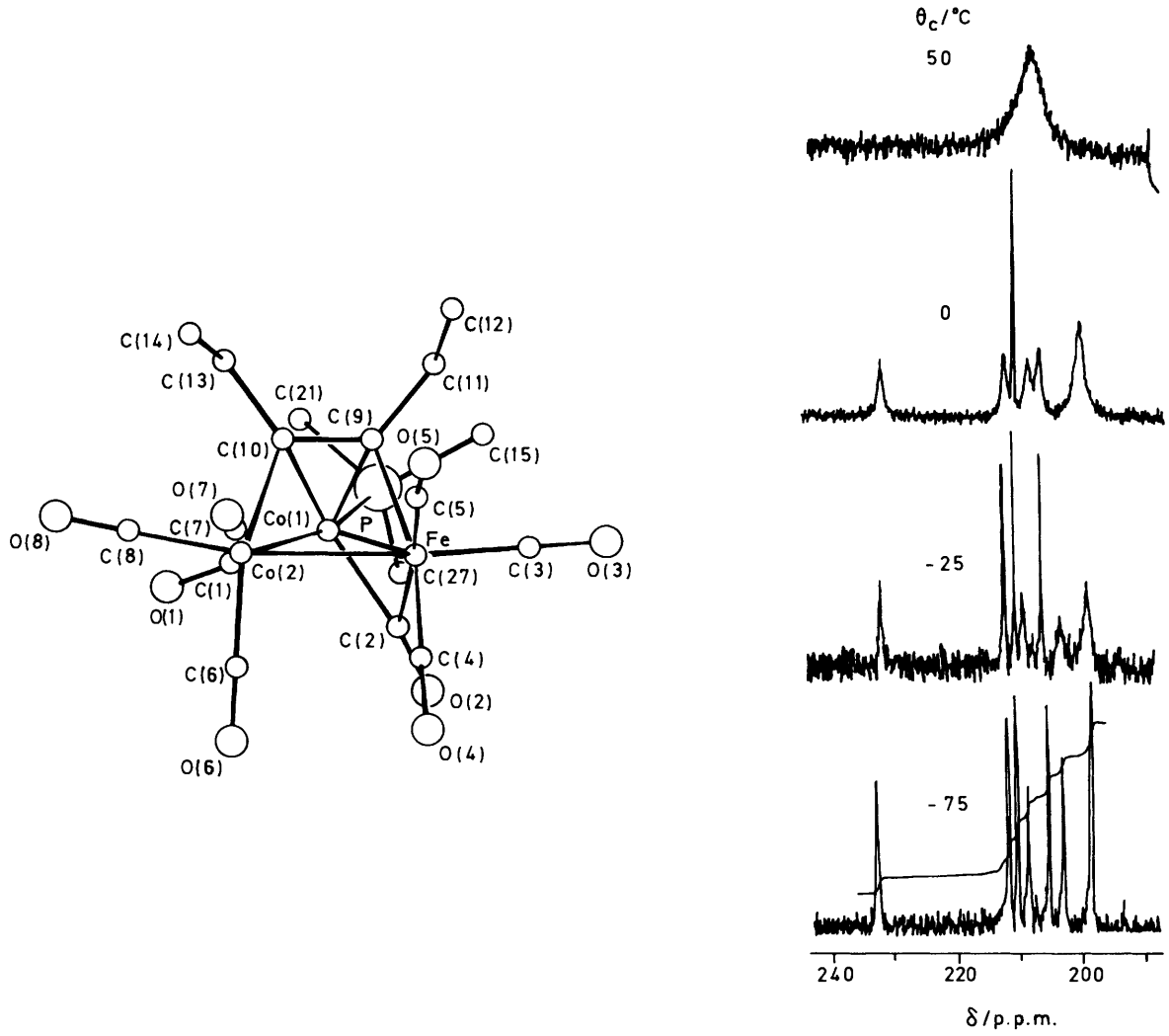

Figure 4. Variable-temperature ^{13}C n.m.r. spectra of a ^{13}CO-enriched sample of $[FeCo_2(CO)_8(PPh_3)(EtC_2Et)]$ (**2b**) recorded at 67.9 MHz in CD_2Cl_2, together with the view of its solid-state structure in the identical orientation of that of complex (**1**)

carbonyls, it is clear that some process is selectively exchanging two of the iron carbonyl resonances. The simplest interpretation is a localized pairwise exchange of such carbonyls; there are precedents for this type of localized scrambling between two of three carbonyls (one axial and one radial) on a $M(CO)_3$ moiety (M = Ru or Os) coupled with an organic ligand motion.[25] An alternative explanation may be a concerted exchange of the carbonyl groups in the metallic plane (merry-go-round) coupled with the alkyne rotation; such a process is analogous to that proposed for the parent compound (**1**) but requires for (**2b**) the rigidity of the $Fe(CO)_3$ moiety [so the axial CO(4) group is not involved in the scrambling] and some degree of phosphine mobility (PPh_3 has been found in an equatorial position in the solid-state structure and may block the merry-go-round process). Finally it is possible to consider a two-centre pairwise exchange process along the FeCo(1) edge coupled with the alkyne rotation where four carbonyls, namely CO(1), CO(2), CO(4), and CO(5) are engaged. This process is very reminiscent of that found on the phosphine-substituted edge of $[Os_3(CO)_{11}(PR_3)]$ (R_3 = Et_3 or Me_2Ph) derivatives, where a two-centre pairwise scrambling of six *in plane* carbonyls (excluding the phosphine and the radial CO perpendicular to the plane) has been shown to take place;[26] obviously in (**2b**) two axial carbonyls are replaced by the co-ordinated alkyne, though in rapid rotation. However an examination of the structure of (**2b**) reveals that the substitution of a CO by PPh_3 has caused deep deformation in the original symmetry in that C(1), C(4), and C(5) deviate from the plane passing through Fe, Co(1), and C(2) (semibridging CO) by 1.143(8), 1.056(8), and 0.119(8) Å respectively. This lack of planarity suggests that the abovesaid mechanism is unlikely for (**2a**)—(**2c**).

Whatever process may operate, at *ca.* 0 °C a further increase in the temperature up to 50 °C causes complete coalescence to a single peak at 208.8 p.p.m., indicating that a total CO exchange over the whole metallic triangle is occurring which certainly involves the alkyne rotation and the breakdown of the phosphine rigidity. The coalescence temperature for this process is inversely proportional to the steric encumbrance of the ligands and follows the order: PPh_3 (**2b**) > PEt_3 (**2a**) > $P(OPh)_3$ (**2d**) > $P(OMe)_3$ (**2c**) > $CNCH_2Ph$ (**2e**) > CO (**1**).

In conclusion, the regiospecific replacement of a CO group on a $Co(CO)_3$ moiety in (**1**) by each ligand employed (ranging from the highly basic PEt_3 to the poorly basic $CNCH_2Ph$) modifies the electron density on the cobalt atom and then stabilizes a different rotamer as previously forecast by Jaouen and co-workers.[6] An alternative explanation of the alkyne reorientation on CO substitution by L as being due to steric repulsion between the ethyl groups of the alkyne and L itself can be

discarded on the basis of molecular models, especially for the less sterically demanding $P(OMe)_3$ and $CNCH_2Ph$ ligands. Similar conclusions on the stereoselectivity during the formation of vinylidene-bridged heterometallic clusters have been recently published by Vahrenkamp and co-workers.[27]

Diphosphine Derivatives.—With the purpose of understanding the modification induced in the parent cluster (**1**) by bidentate ligands, we treated $[FeCo_2(CO)_9(EtC_2Et)]$ (**1**) with dppe, dppp, and dppb respectively. Again the use of the $[\{Fe(CO)_2(PPh_3)(SMe)\}_2]$ catalyst allows the reactions to occur quickly at room temperature and afford a single product in reasonable yield (see Experimental section). The i.r. spectra of the products, (**3a**)—(**3c**), are very close to that of $[FeCo_2(CO)_8(PPh)_3(EtC_2Et)]$ (**2b**). The ^{31}P n.m.r. spectra exhibit a single resonance in a region typical of co-ordinated phosphorus, from room temperature down to −50 °C (see Table 1). These features strongly suggest a dimeric structure for these compounds, *i.e.* $[\{FeCo_2(CO)_8(EtC_2Et)\}_2\{\mu\text{-}PPh_2(CH_2)_nPPh_2\}]$ [n = 2, dppe, (**3a**); n = 3, dppp, (**3b**); n = 4, dppb, (**3c**)]. Similar compounds, in which a bidentate ligand bridges two cluster units, have been previously identified by spectroscopic studies, *i.e.* $[\{Ru_3(CO)_{11}\}_2(\mu\text{-dppe})]$,[28] $[\{Ru_4H_4(CO)_4\}_2(\mu\text{-dppe})]$,[29] $[\{Co_4(CO)_{11}\}_2(\mu\text{-dppe})]$,[30] $[\{Co_3(CO)_8(CCl)\}_2\{Ph_2P(CH_2)_n\text{-}PPh_2\}]$[31] ($n$ = 2—4) and by an *X*-ray investigation on $[\{Co_3(CO)_8(CPh)\}_2(\mu\text{-dppe})]$.[32]

Further support to the dimeric nature of these derivatives comes from their variable-temperature ^{13}C n.m.r. spectra. The low-temperature limiting spectra of ^{13}CO-enriched samples of (**3a**)—(**3c**) are very similar to those of complexes (**2a**)—(**2c**). For example, in the case of $[\{FeCo_2(CO)_8(EtC_2Et)\}_2(\mu\text{-dppp})]$ (**3b**) the spectrum at −40 °C exhibits seven resonances at 231.0 (apparent doublet), 212.0, 210.7, 208.2, 206.3, 202.9, and 199.9 p.p.m. in the intensity ratio 1:1:1:1:1:1:2; interestingly the semibridging CO resonance is actually split into two very close peaks at 232.3 and 231.4 p.p.m. respectively (Figure 5). Provided that the carbonyl exchange process within each cluster unit is frozen out at this temperature as well as the fluxionality of the bridging diphosphine, the splitting in the semibridging resonance may derive from the presence in solution of a mixture of two isomers in a 1:1 ratio having a *cis–trans* relationship (Figure 5). On increasing the temperature a dynamic process identical to that discussed for (**2a**)—(**2c**) takes place, which is likely coupled with the rotation of the bidentate ligand around its axis, and affords the magnetic equivalence of all the CO groups at *ca.* 40 °C for (**3a**)—(**3c**).

Interestingly enough, the splitting (Δ) of the two semibridging carbonyl resonances depends on the length of the organic chain of the $PPh_2(CH_2)_nPPh_2$ ligand: (**3a**), n = 2, Δ = 1.4; (**3b**), n = 3, Δ = 0.9; (**3c**), n = 4, Δ = 0.5 p.p.m.; the largest distance between the two cluster moieties in the dimer corresponds to the smallest difference in magnetic environment of the semibridging carbonyls. This seems to lead additional support to the occurrence of the *cis–trans* isomeric mixture, which should be sensitive to the length of the bridging bidentate ligand.

Experimental

General.—The parent compound $[FeCo_2(CO)_9(EtC_2Et)]$ (**1**) and the catalyst $[\{Fe(CO)_2(PPh_3)(SMe)\}_2]$ were prepared according to the published procedure.[11,17] The ligands were commercial products of the highest purity available and were used as received. All manipulations were carried out under nitrogen.

Elemental analyses were carried out on a F and M model 185 CHN analyzer and Perkin-Elmer 303 atomic absorption spectrometer.

Infrared spectra were recorded on a Perkin-Elmer 580 B spectrometer, the ^1H, ^{13}C, and ^{31}P n.m.r. spectra on a JEOL 270/89 instrument at 270.0, 67.8, and 109.3 MHz respectively; chemical shifts are reported in p.p.m. downfield from the standard $SiMe_4$ (^1H, ^{13}C) or 85% H_3PO_4 (^{31}P). Mass spectra for (**2c**) and (**2a**) were obtained on an AEI MS 12 instrument.

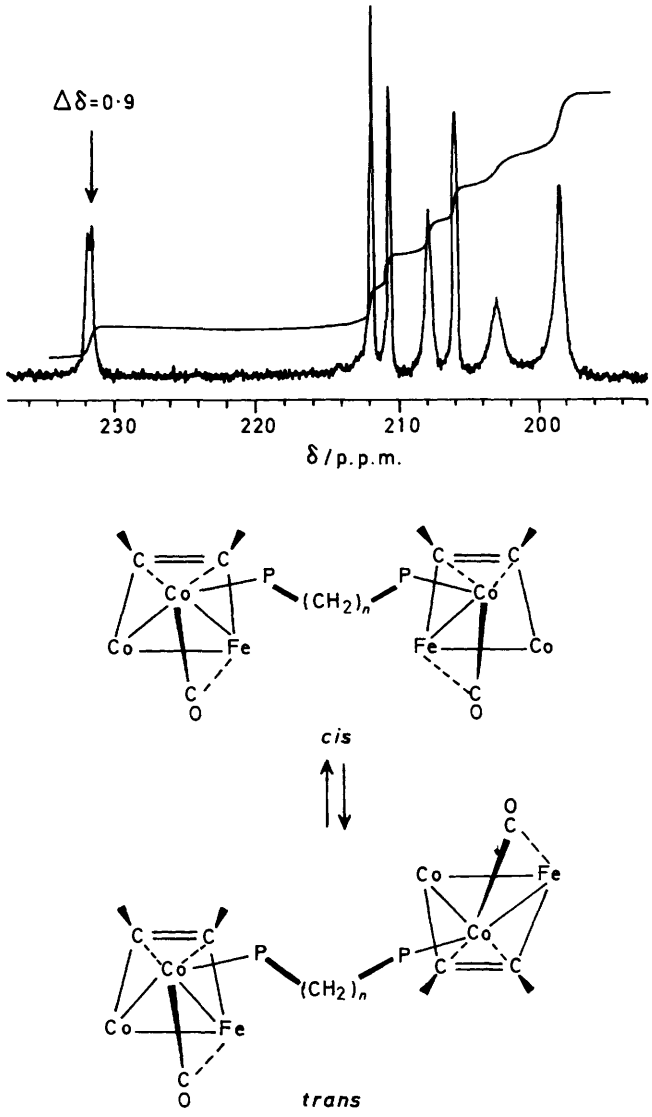

Figure 5. Low-temperature (−40 °C) ^{13}C n.m.r. limiting spectrum of a ^{13}CO-enriched sample of $[\{FeCo_2(CO)_8(EtC_2Et)\}_2\{Ph_2P(CH_2)_3\text{-}PPh_2\}]$ (**3b**) recorded at 67.9 MHz in $CDCl_3$ together with the proposed mechanism of *cis–trans* interconversion (CO groups and Et substituents have been omitted for clarity)

Reaction of $[FeCo_2(CO)_9(EtC_2Et)]$ (**1**) *with Phosphine* L (PEt_3 *or* PPh_3).—In a typical run (**1**) (2.0 g, 3.9 mmol), the appropriate phosphine L (3.9 mmol), and the catalyst $[\{Fe(CO)_2(PPh_3)(SMe)\}_2]$ (85 mg, 0.4 mmol) were stirred in n-hexane (100 cm^3) in a two-necked flask wrapped in aluminium foil at room temperature under N_2 for 2 h. The solvent was removed under reduced pressure and the brown residue dissolved in CH_2Cl_2 and chromatographed on a silica column. Elution was carried out with light petroleum (b.p. 40—70 °C), which eluted unreacted (**1**) (5%); elution was repeated with light petroleum–CH_2Cl_2 (3:1 v/v), which eluted $[FeCo_2(CO)_8L(EtC_2Et)]$ [L = PEt_3 (**2a**), green solid, 90%; L = PPh_3 (**2b**), dark green solid, 80%].

Reaction of $[FeCo_2(CO)_9(EtC_2Et)]$ (**1**) *with Phosphite* L [$P(OPh)_3$ *or* $P(OMe)_3$].—A solution of the appropriate phosphite L (3.9 mmol in 2 cm^3 of n-hexane) was added dropwise to a hexane solution of (**1**) (2.0 g) and $[\{Fe(CO)_2(PPh_3)(SMe)\}_2]$ (85 mg) and the mixture stirred at room temperature under N_2 for 5 h. Similar separation work-up as above gave unreacted (**1**) (5%) and $[FeCo_2(CO)_8L(EtC_2Et)]$ [L = $P(OMe)_3$ (**2c**), brown oil, 70%; L = $P(OPh)_3$ (**2d**), green-brown oil, 65%].

Reaction of $[FeCo_2(CO)_9(EtC_2Et)]$ (**1**) *with* $CNCH_2Ph$.—Complex (**1**) (2.0 g) and $[\{Fe(CO)_2(PPh_3)(SMe)\}_2]$ (85 mg) were dissolved in n-hexane (100 cm^3) and $CNCH_2Ph$ (1.3 cm^3, 3.9 mmol) added dropwise. The mixture was stirred for 2 h at room temperature under N_2. Separation work-up gave unreacted (**1**) (10%), $[FeCo_2(CO)_8(CNCH_2Ph)(EtC_2Et)]$ (**2e**) (brown solid, 70%), and a yellow-orange complex (10%) as yet not characterized.

Reaction of $[FeCo_2(CO)_9(EtC_2Et)]$ (**1**) *with Diphosphine* L–L (*dppe, dppp, or dppb*).—Complex (**1**) (2.0 g), $[\{Fe(CO)_2(PPh_3)(SMe)\}_2]$ (85 mg), and the appropriate diphosphine L–L (3.9 mmol) were dissolved in n-hexane (100 cm^3) and the mixture stirred at ambient temperature under N_2 for 4 h. T.l.c. separation work-up and subsequent crystallization of the sole dark green band in heptane–$CHCl_3$ (3:1, v/v) gave the dimeric complexes $[\{FeCo_2(CO)_8(EtC_2Et)\}_2(L–L)]$ [L–L = dppe (**3a**), 60%; L–L = dppp (**3b**), 70%; L–L = dppb (**3c**), 75%] as green crystals.

Crystal-structure Determination of $[FeCo_2(CO)_8(PPh_3)(EtC_2Et)]$ (**2b**).—Black crystals of (**2b**) suitable for *X*-ray analysis were obtained from a saturated n-heptane–$CHCl_3$ (9:1 v/v) solution kept at −20 °C under N_2.

Crystal data. $C_{32}H_{25}Co_2FeO_8P$, M = 742.23, triclinic, a = 10.690(4), b = 16.267(8), c = 9.457(5) Å, α = 95.01(3), β = 107.55(3), γ = 89.23(2)°, U = 1 562(1) $Å^3$ (by least-squares refinement from the θ values of 28 reflections accurately measured, λ = 0.710 69 Å), space group $P\bar{1}$, Z = 2, D_c = 1.578 g cm^{-3}, $F(000)$ = 752. A flattened prismatic crystal of approximate dimensions 0.1 × 0.35 × 0.64 mm was used for the structural analysis, μ(Mo-K_α) = 16.05 cm^{-1}. No correction for the absorption effect was applied because of the low absorbance of the sample.

Data collection and processing. Siemens AED diffractometer, θ/2θ mode, niobium-filtered Mo-K_α radiation; all reflections in the range $3 \leqslant \theta \leqslant 27°$ were measured. Of 6 760 independent reflections 4 165, having $I \geqslant 2\sigma(I)$, were considered observed and used in the analysis.

Structure analysis and refinement. Direct and Fourier methods, full-matrix least-squares refinement with anisotropic thermal parameters in the last cycles for all the atoms excepting the carbon atoms of the phenyl rings. At this stage the R and R' values were 0.0626 and 0.0716 respectively. Although the difference in the *X*-ray scattering power for Fe and Co is very small, the correct position of the iron atom in the cluster was confirmed by different refinements carried out by placing the iron atom in the other two possible positions of the metallic triangle, *i.e.* with Fe replacing Co(1) (R and R' 0.0646 and 0.0742) or with Fe replacing Co(2) (R and R' 0.0644 and 0.0737) respectively. The hydrogen atoms, not all clearly localized in the final ΔF map, were placed at their geometrically calculated positions and introduced in the final calculations with isotropic thermal parameters. The weighting scheme used in the last cycles of refinement was $w = K/[\sigma^2(F_o) + gF^2_o|^{-1}$ with K = 0.8679 and g = 0.1082. Final R and R' values were 0.0563 and 0.0601 respectively. The SHELX system of computer programs was used.[33] Atomic scattering factors, corrected for the anomalous dispersion of Co, Fe, and P were taken from ref. 34.

Table 4. Fractional atomic co-ordinates (× 10^4) with e.s.d.s in parentheses for the non-hydrogen atoms of complex (**2b**)

Atom	*X/a*	*Y/b*	*Z/c*
Co(1)	3 540(1)	2 239(1)	1 295(1)
Co(2)	1 177(1)	2 364(1)	114(1)
Fe	2 389(1)	3 190(1)	2 659(1)
P(1)	5 678(2)	2 075(1)	1 768(2)
O(1)	3 094(7)	692(4)	−513(8)
O(2)	3 633(6)	1 636(4)	4 096(7)
O(3)	4 205(7)	3 992(5)	5 360(7)
O(4)	759(8)	2 471(5)	4 250(8)
O(5)	866(6)	4 662(4)	1 926(8)
O(6)	346(8)	1 039(5)	1 566(9)
O(7)	−1 020(6)	3 481(4)	−517(8)
O(8)	440(8)	1 507(5)	−2 893(8)
C(1)	3 230(7)	1 302(4)	210(8)
C(2)	3 468(7)	2 008(4)	3 092(7)
C(3)	3 524(8)	3 686(5)	4 279(9)
C(4)	1 370(8)	2 745(5)	3 616(8)
C(5)	1 460(7)	4 072(5)	2 206(9)
C(6)	646(8)	1 557(5)	1 005(10)
C(7)	−144(8)	3 065(5)	−248(9)
C(8)	755(8)	1 814(5)	−1 751(10)
C(9)	3 248(6)	3 472(4)	1 129(7)
C(10)	2 553(6)	3 067(4)	−199(7)
C(11)	4 259(7)	4 161(4)	1 391(8)
C(12)	3 663(10)	5 008(4)	1 161(12)
C(13)	2 581(8)	3 253(5)	−1 726(8)
C(14)	1 346(9)	3 748(6)	−2 520(10)
C(15)	6 724(6)	2 921(4)	2 828(7)
C(16)	6 738(8)	3 115(5)	4 297(9)
C(17)	7 516(9)	3 760(6)	5 165(10)
C(18)	8 234(9)	4 215(6)	4 562(10)
C(19)	8 227(9)	4 037(5)	3 068(10)
C(20)	7 487(7)	3 388(4)	2 244(8)
C(21)	6 146(6)	1 883(4)	70(7)
C(22)	5 693(8)	2 402(5)	−1 036(9)
C(23)	6 004(9)	2 301(6)	−2 373(11)
C(24)	6 787(8)	1 643(5)	−2 582(9)
C(25)	7 237(9)	1 124(6)	−1 502(10)
C(26)	6 935(7)	1 240(5)	−156(9)
C(27)	6 395(6)	1 215(4)	2 850(7)
C(28)	7 727(7)	1 211(4)	3 563(8)
C(29)	8 298(9)	538(5)	4 334(10)
C(30)	7 542(8)	−118(5)	4 423(9)
C(31)	6 220(8)	−99(5)	3 735(9)
C(32)	5 618(7)	546(4)	2 929(8)

All calculations were performed on the CRAY X-MP/12 computer of the Centro di Calcolo Elettronico Interuniversitario dell'Italia Nord-Orientale, Bologna, and on the GOULD-SEL 32/77 computer of the Centro di Studio per la Strutturistica Diffrattometrica del C.N.R., Parma. Final atomic co-ordinates for the non-hydrogen atoms are given in Table 4.

Data available from the Cambridge Crystallographic Data Centre are as follows: thermal parameters, H-atom co-ordinates, remaining bond lengths and angles, interatomic contacts.

N.M.R. Samples.—Compounds (**2a**)—(**2e**) and (**3a**)—(**3c**) are quite air-sensitive and must be handled under an inert atmosphere (N_2), especially during the preparation of an n.m.r. sample, in order to avoid their partial decomposition to paramagnetic species. However, these species can be easily eliminated on passing the solution through a small cellulose column in N_2 flux. The ^{13}C n.m.r. spectra of all the derivatives have been obtained by using ^{13}CO-enriched samples synthesized in an analogous manner starting from ^{13}CO-enriched (**1**).

Enrichment of $[FeCo_2(CO)_9(EtC_2Et)]$ (**1**). For each enrichment, complex (**1**) (200 mg) in cyclohexane (100 cm^3) was placed in a sealed ampoule under *ca.* 0.2 atm ^{13}CO (Monsanto Corp.); the vessel was wrapped in aluminium foil and kept in a thermostatted water-bath at 60 °C for 5 d. The ^{13}CO content was estimated as being in the range 15—20% by matching the experimentally observed mass spectral isotope pattern with the calculated values.

Acknowledgements

We gratefully thank the Italian MPI for financial support and Dr. E. Rosenberg (California State University) for useful suggestions.

References

1 R. Ugo, *Catal. Rev.*, 1975, **11**, 225; E. L. Muetterties, T. N. Rhodin, E. Band, C. F. Brucker, and W. R. Pretzer, *Chem. Rev.*, 1979, **79**, 91.
2 J. F. Blount, L. F. Dahl, C. Hoogzand, and W. Hubel, *J. Am. Chem. Soc.*, 1966, **88**, 292.
3 A. J. Deeming, S. Hasso, and M. Underhill, *J. Chem. Soc., Dalton Trans.*, 1975, 1614.
4 M. G. Thomas, E. L. Muetterties, R. O. Day, and V. W. Day, *J. Am. Chem. Soc.*, 1976, **98**, 4645.
5 B. E. R. Schilling and R. Hoffmann, *J. Am. Chem. Soc.*, 1979, **101**, 3456.
6 J. F. Halet, J. Y. Saillard, R. Lissillour, M. J. McGlinchey, and G. Jaouen, *Inorg. Chem.*, 1985, **24**, 218.
7 D. Osella, R. Gobetto, P. Montangero, P. Zanello, and A. Cinquantini, *Organometallics*, 1986, **5**, 1247.
8 G. Granozzi, E. Tondello, M. Casarin, S. Aime, and D. Osella, *Organometallics*, 1983, **2**, 430; V. Busetti, G. Granozzi, S. Aime, R. Gobetto, and D. Osella, *ibid.*, 1984, **3**, 1510; S. Aime, R. Bertoncello, V. Busetti, R. Gobetto, G. Granozzi, and D. Osella, *Inorg. Chem.*, 1986, **25**, 4004.
9 D. M. P. Mingos, *Acc. Chem. Res.*, 1984, **17**, 311.
10 M. R. Churchill, C. Bueno, and J. Wasserman, *Inorg. Chem.*, 1982, **21**, 640; L. Busetto, M. Green, B. Hessner, J. A. K. Howard, J. C. Jeffrey and F. G. A. Stone, *J. Chem. Soc., Dalton Trans.*, 1983, 519.
11 S. Aime, L. Milone, D. Osella, A. Tiripicchio, and A. M. Manotti-Lanfredi, *Inorg. Chem.*, 1982, **21**, 501.
12 P. Braunstein, J. Rose, and O. Bars, *J. Organomet. Chem.*, 1983, **252**, C101; E. Roland, W. Bernhardt, and H. Vahrenkamp, *Chem. Ber.*, 1985, **118**, 2858.
13 F. A. Cotton, *Prog. Inorg. Chem.*, 1976, **21**, 1.
14 F. W. B. Einstein, K. G. Tyers, A. S. Tracey, and D. Sutton, *Inorg. Chem.*, 1986, **25**, 1631.
15 C. G. Pierpont, *Inorg. Chem.*, 1977, **16**, 636.
16 J. Evans and G. S. McNulty, *J. Chem. Soc., Dalton Trans.*, 1981, 2017.
17 S. Aime, M. Botta, R. Gobetto, and D. Osella, *Organometallics*, 1985, **4**, 1475.
18 S. Aime, L. Milone, R. Rossetti, and P. L. Stanghellini, *Inorg. Chim. Acta*, 1977, **25**, 103.
19 S. Aime, L. Milone, D. Osella, and A. Poli, *Inorg. Chim. Acta*, 1978, **30**, 45.
20 S. Aime, D. Osella, L. Milone, and A. Tiripicchio, *Polyhedron*, 1983, **2**, 77.
21 R. Gobetto, S. Aime, M. Botta, and D. Osella, unpublished work.
22 C. A. Tolman, *Chem. Rev.*, 1977, **77**, 313.
23 D. A. Roberts and G. L. Geoffroy, in 'Comprehensive Organometallic Chemistry,' eds. G. Wilkinson, F. G. A. Stone, and E. W. Abel, Pergamon Press, Oxford, 1982, ch. 40.
24 S. Aime, G. Gervasio, L. Milone, and E. Rosenberg, *Transition Met. Chem.*, 1977, **1**, 177.
25 S. Aime, R. Gobetto, D. Osella, L. Milone, and E. Rosenberg, *Organometallics*, 1982, **1**, 640.
26 B. F. G. Johnson, J. Lewis, B. E. Reichert, and K. T. Schorpp, *J. Chem. Soc., Dalton Trans.*, 1976, 1403; A. J. Deeming, S. Donovan-Mtunzi, and S. E. Kabir, *J. Organomet. Chem.*, 1985, **281**, C43; A. J. Deeming, S. Donovan-Mtunzi, S. E. Kabir, and P. J. Manning, *J. Chem. Soc., Dalton Trans.*, 1985, 1037.
27 C. von Schnering, T. Albiez, W. Bernhardt, and H. Vahrenkamp, *Angew. Chem., Int. Ed. Engl.*, 1986, **25**, 479.
28 M. L. Bruce, T. W. Hambley, B. K. Nicholson, and M. R. Snow, *J. Organomet. Chem.*, 1982, **235**, 83.
29 M. I. Bruce, O. B. Shawkataly, and M. L. Williams, *J. Organomet. Chem.*, 1985, **287**, 127.
30 S. Aime, R. Gobetto, G. Jannon, and D. Osella, *J. Organomet. Chem.*, 1986, **309**, C51.
31 S. Aime, M. Botta, R. Gobetto, D. Osella, and L. Milone, *Gazz. Chim. Ital.*, in the press.
32 A. J. Downard, B. H. Robinson, and J. Simpson, *Organometallics*, 1986, **5**, 1123.
33 G. M. Sheldrick, SHELX, System of Computing Programs, University of Cambridge, 1976.
34 'International Tables for *X*-Ray Crystallography,' Kynoch Press, Birmingham, 1974, vol. 4.

Received 15*th April* 1987; *Paper* 7/688